Journal of Power Sources, 36 (1991) 137–153

The physical and chemical state of phosphoric acid fuel cell assemblies after long term operation: surface and near-surface analysis

M. T. Paffett*, W. Hutchinson, J. D. Farr, P. Papin, J. G. Beery[a] and S. Gottesfeld

Chemical and Laser Sciences Division, [a]Electronics Research Group, Los Alamos National Laboratory, Los Alamos, NM 87545 (U.S.A.)

J. Feret

Westinghouse Electric Corporation, Box 10864, Pittsburgh, PA 15236 (U.S.A.)

(Received September 30, 1990; in revised form April 15, 1991)

Abstract

An attempt was made to correlate performance losses with materials compatibility and compositional changes in phosphoric acid fuel cell (PAFC) electrode assemblies as a function of operation time. Westinghouse PAFC stacks were run under a constant operating regime and portions of some of the single cells were analyzed after stack operation for 5000 and 16 000 h along with appropriate reference samples. The PAFC assemblies were disassembled, sectioned where appropriate and analyzed using scanning and transmission electron microscopy (SEM and TEM), Rutherford backscattering spectroscopy (RBS), electron microprobe analysis (EMP), and X-ray photoelectron spectroscopy (XPS). The profiles of the Pt catalyst in both the anode and the cathode layer did not show any preferential loss or peaking. The most pronounced change in cell composition detected following stack operation for 5000 and 16 000 h was the increase in Pt/C ratio, that was related to loss of carbon from the cathode electrocatalyst. In contrast, the anode catalyst layer maintains the same ratio of Pt:C following 16 000 h of operation. The loss of carbon is thought to occur by an electrochemical mechanism and is enhanced at the higher potentials experienced by the air cathode in the fuel cell. In addition, TEM results clearly demonstrate the well recognized phenomenon of Pt particle agglomeration in the cathode catalyst layer, which is seen to be quite substantial after 5000 h of stack operation. This behavior was not observed at the anode electrocatalyst layer. The mechanical integrity of the assemblies was found to be quite satisfactory after 5000 h, but much less so after 16 000 h. Questions regarding carbon and Pt corrosion, Pt migration, and the chemical and physical integrity of the PAFC structures are addressed and are all postulated to be contributing to the observed cell performance losses.

Introduction

In the development of phosphoric acid fuel cell (PAFC) systems there have been several scientific and engineering obstacles to overcome if this technology is to be competitive with other more conventional electrical energy

*Author to whom correspondence should be addressed.

0378-7753/91/$3.50

sources. One of the key problems that is crucial for this technology to succeed is a stable long term operation of the PAFC. Within the operational goals of the Westinghouse PAFC program a degradation in cell voltage at a constant load of 267 mA per cm^2 of 4 mV/1000 h is now considered feasible [1]. This performance loss is a significant improvement over previous performance degradation results [2]. However, an even lower degradation rate during long term operation is a desirable goal. Specifically, questions regarding carbon corrosion, Pt corrosion and Pt migration through the PAFC assembly have all been postulated to contribute to the observed cell performance loss. The present body of work attempts to assess analytically several materials degradation problems as they occur in the PAFC. In the interest of addressing these issues directly, we have examined the surface and near-surface regions of a series of Westinghouse PAFC assemblies that have been run under an essentially continuous power load for various time intervals up to 16 000 h. We have directly addressed the pertinent questions listed above and present the results herein.

The experimental approach to these issues has been as follows: Westinghouse PAFC stacks were run under a constant operating regime. The operating regime has been amply documented [1] and is briefly summarized as follows. The cell portions were specific sectioned electrode assemblies from an air cooled Westinghouse phosphoric acid fuel cell that was run at 190 ± 10 °C using synthetic reformate gas at a pressure of 70 psia. Cells were never exposed at open circuit to hot operating conditions. Overall cell performance (*I–V* curves) of the sectioned and analyzed portions was typical of that previously published [1]. Typical ranges of cell voltage and current density during testing were 200–270 mA cm^{-2} and 590–690 mV. Portions of cell assemblies were sent to LANL for analysis after stack operation for 5000 and 16 000 h along with appropriate reference samples. The PAFC assemblies were disassembled, sectioned where appropriate and analyzed using scanning and transmission electron microscopy (SEM and TEM), Rutherford backscattering spectroscopy (RBS), electron microprobe analysis (EMP) and X-ray photoelectron spectroscopy (XPS). The information obtained and the strengths and weaknesses of each of these techniques is briefly summarized at the beginning of the relevant section. The SEM results will be presented together with the EMP results because both of these analyses were run sequentially in the same instrument.

EMP and SEM results

Electron microprobe analysis (EMP) allows one to quantify the near surface region of metallographic specimens for elements of $Z > 3$. The instrumentation involves exciting the near-surface volume with 10–25 KeV electrons and analyzing the intensity of the characteristic X-ray emission from the elements present in the sample. The method provides excellent lateral spatial analysis (0.1 μm resolution) of elements detected with routine

detection limits in the order of 0.1 wt.%. The excitation volume, the X-ray fluorescence cross section, and a variety of instrumental detection and efficiency parameters all influence the measured intensity of the observed X-ray emission [3]. The PAFC assembly samples, examined by EMP, were mounted edge on end in metallographic epoxy, polished to reveal the distinct layers in the PAFC assembly, and then washed with water and evacuated in a vacuum oven. The latter step was necessary to achieve an adequate background pressure in the EMP (outgassing from the phosphoric acid and residual water was the primary problem). In the present case a 10 μm^2 15 KeV electron beam was scanned across the cross section of the fuel cell assemblies and the X-ray emission from the elements present in greater than 1 wt.% was analyzed. Secondary electron micrographs (SEM) were also taken of selected PAFC cross sections. In most cases the distinct layers making up the assemblies are easily identified and are labeled in Figs. 1, 2, 5, 6 and 8. Image maps of targeted elements are shown along with the respective SEM photos. The element maps are constructed from the output of either the wavelength or energy dispersive detector(s) and contain some noise associated with these measurements. For the lateral, semi-quantitative line plots the background noise was subtracted to derive the apparent concentration (in wt.%). PAFC electrode assemblies are not the most ideal structures for this type of analysis because of their fairly porous, extremely rough structure. Because of the non-ideal nature of the surface the concentrations should be viewed as only semi-quantitative. However, the EMP technique does allow one to assess the extent of Pt migration, non-uniformity of Pt loading, and other materials problems that arise during long term operation.

In Fig. 1, a SEM of a sectioned, reference (unused) anode is shown along with a Pt X-ray map for the same region. The SEM clearly shows the nice delineation between the porous carbon backing and the rolled electrocatalyst layer. Note also that the Pt distribution is quite uniform within the electrocatalyst layer and matches the SEM demarcation exactly. The non-zero intensity of the image obtained in the area of the backing is caused by background (noise) effects. In Fig. 2, a SEM of the reference (unused) cathode is shown denoting the various layers comprising the cathode assembly as received. Note that the mat layer, the SiC matrix, the rolled electrocatalyst layer, and the porous carbon backing are all clearly delineated and show extremely good edge retention following sample preparation. The layer thicknesses are also consistent with reported values [2]. Wavelength dispersive elemental maps of the cathode structure demonstrated very good edge retention with the Pt distribution nearly identical to that seen in the anode structure and are not shown for brevity. In Figs. 3 and 4, line scans taken over the electrocatalytic layers and the regions immediately adjacent to them are presented for the same electrodes shown in Figs. 1 and 2, respectively. For the reference anode the weight percent concentration of the elements C, O, F (top half of Fig. 3) Cl, P and Pt (bottom half of Fig. 3) is shown as a function of position across the porous backing and the electrocatalytic layer. Note that the Pt concentration varies somewhat across the electrocatalyst

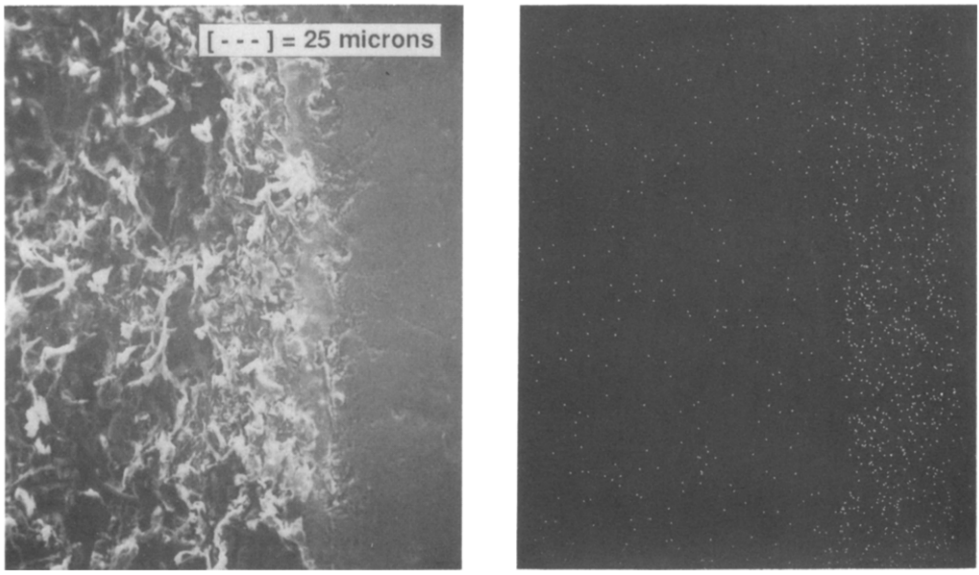

(a) (b)

Fig. 1. (a) Secondary electron micrograph (SEM) of a cross-sectioned reference anode; (b) Pt X-ray fluorescence image recorded over the same region as shown in (a).

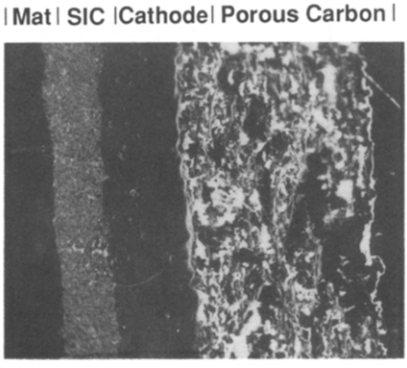

Fig. 2. SEM of a cross-sectioned reference cathode assembly at 50× magnification. Parts of the electrode assembly are labeled.

layer but in general runs around 3–4 wt.%. This value is markedly lower than the stated nominal value of 10% weight loading for the electrocatalytic layer and serves to point out the difficulties of quantification on very porous, rough samples. Due to this limitation the reported numbers should be directly compared with the reference samples for some understanding of how the Pt and C concentrations vary in a relative sense. The C concentration runs at 75 ± 5 wt.% for both the anode and cathode and will prove to be a key number for comparison to the used electrode assemblies. Note that the C concentration from the EMP analysis is a combined value from the support

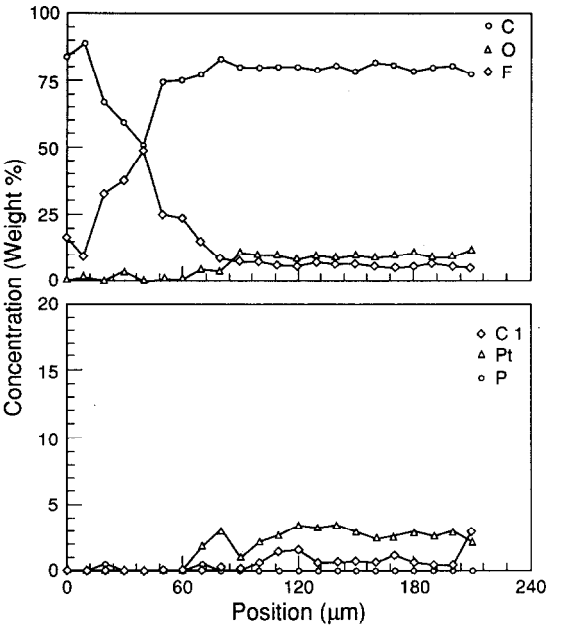

Fig. 3. Concentrations in wt.% recorded over a line scan of the reference anode (Fig. 1).

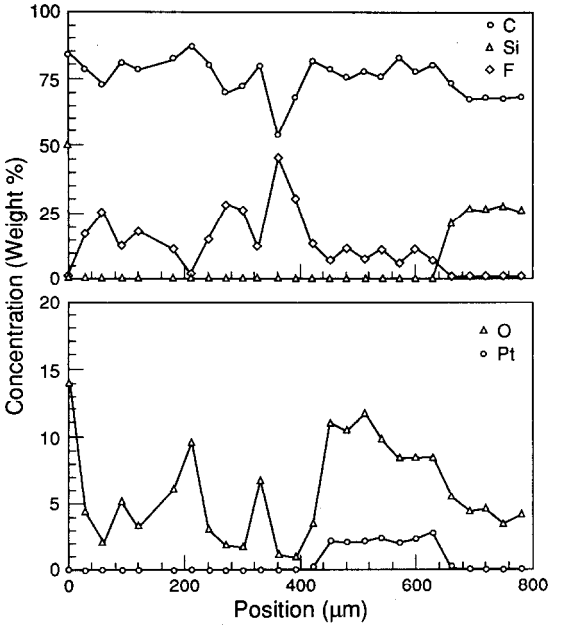

Fig. 4. Concentrations in wt.% recorded over a line scan of the assembly shown in Fig. 2 (cathode reference).

and the Teflon constituents. Also of note, is the higher concentration of F in the porous backing particularly that of the anode structure. The statistical variation in elemental concentration is quite pronounced in the porous backing and is largely due to the very rough, spongy nature of the substrate. Some Cl is observed in the electrocatalyst layer. The origin of this Cl is not entirely clear, although some residual contamination from the potting compound (epoxy) is suspect. Figure 4 displays the elemental line scans from the reference cathode performed across the layers shown in Fig. 2. The Pt weight concentration is approximately 2–3% and, again, the F concentration is slightly higher in the porous backing. In general, the two reference electrode assemblies appear to be very close in elemental concentrations.

Samples labeled 2-4 and 6-4 were received after being operated approximately 5000 h in a Westinghouse PAFC stack. For brevity, only the 2-4 data set is presented in this report. Analysis of the 6-4 electrode assembly produced analogous results. In Fig. 5, a SEM of a cross-sectioned 2-4 cell assembly is shown with the assembly layers appropriately labeled. Note that the edge relief is still fairly good although some retraction of the middle sections (anode, mat, SiC and cathode) is occurring. Figure 6 contains a SEM enlargement of the cathode–SiC–mat assembly, along with a Pt X-ray map. The X-ray map clearly indicates that the Pt distribution is still uniform in the cathode electrocatalyst layer with no noticeable loss of Pt at the front edge of the layer. Questions regarding Pt agglomeration are addressed in the TEM results section below. Figure 7 contains the elemental (C, O, P, F, Pt) line scans for the PAFC 2-4 electrode assembly sample shown in Fig. 5. For both the anode and cathode layers the Pt weight concentration is running 2–5% with the concentration slightly higher in the cathode layer.

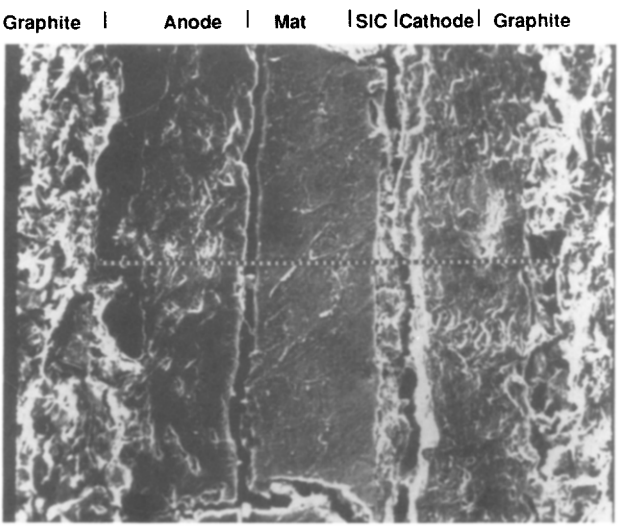

Fig. 5. SEM of fuel cell electrode assembly 2-4 operated for 5000 h. Portions of the assembly are denoted at the top of the Fig.

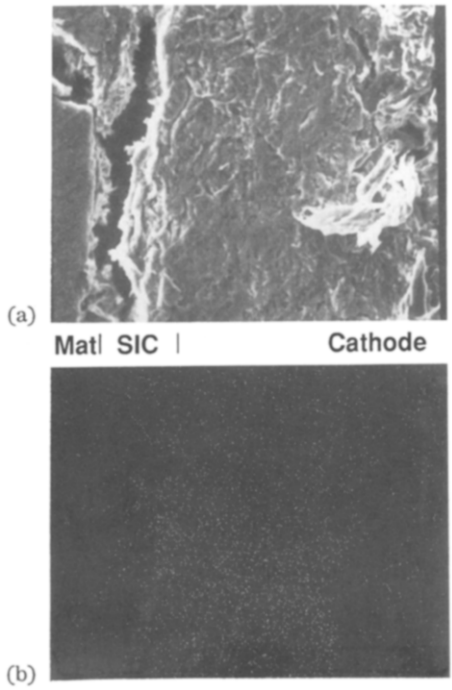

Fig. 6. (a) Expanded view of the mat, SiC and cathode layers in electrode assembly 2-4. (b) Pt X-ray fluorescence image of the same region as (a).

The sharp drop in C, O and F at the interface regions is largely due to the void noted in the SEM photo. This void is apparently caused by partial delamination of adjoining layers in the assembly. In general, the elemental distributions appear uniform except in those regions where the electron beam is sampling void regions. Across the anode and cathode regions of the 2-4 assemblies the C weight concentration varies from 45–65%, a value considerably below that for either reference electrocatalyst layer. The Pt/C ratio averages 0.06 ± 0.005, and 0.11 ± 0.05 in the 2-4 anode and cathode regions, respectively. These numbers compare with values of 0.04 and 0.035 for the reference anode and cathode regions, respectively.

A series of PAFC assemblies run for 16 000 h labeled 8-3, 8-5, 8-7 and 9-8 were analyzed in the same manner as those described above. Again for brevity only one set of results for the 16 000 h set will be described. In general, the results were consistent among the sets and details regarding those assemblies not described are available upon request. Starting with the SEM photo of the 8-3 PAFC electrode assembly (Fig. 8) one notes that the overall middle section has thinned considerably and in some of the assemblies (not shown) has lost a lot of the mechanical integrity. The mechanical integrity assists in maintaining good edge retention in the metallographic preparation of the cross-sectional mounts. For most of the 16 000 PAFC electrode assemblies the SiC layer has diminished to such a degree as to be non-

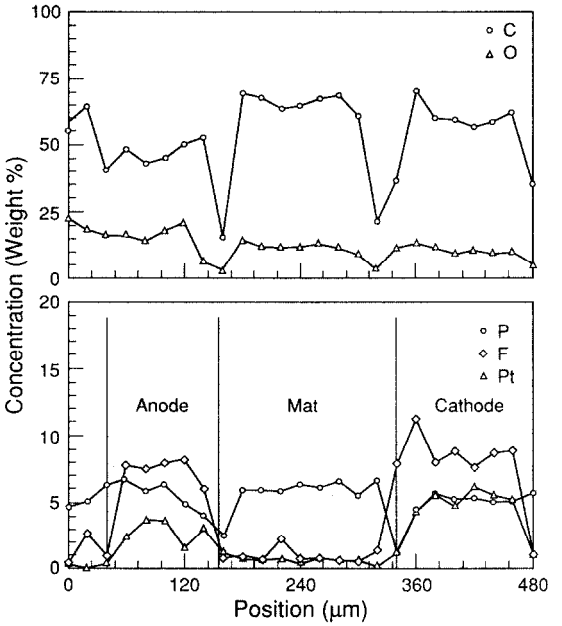

Fig. 7. Weight concentrations determined from the X-ray fluorescence along the line scan denoted in Fig. 5. Portions of the electrode assembly are denoted on the Fig.

distinct. This is brought out in the middle third of Fig. 8 where a Si X-ray map is shown of the same region that the SEM photo is recorded from. Some regions of localized Si are seen, but in general the layer has lost most of its integrity. This loss of SiC after long term operation is puzzling and at this time we have no clear cut explanation for its disappearance other than corrosion. In the bottom third of Fig. 8 the Pt X-ray fluorescence map is shown over the same SEM region. As seen in the prior electrode assemblies the Pt distribution appears uniform with no noticeable Pt loss at the cathode and no replating of the Pt occurring at the anode. A higher concentration of Pt appears in both the cathode and the anode, and is also evident in the elemental line scans that follow in Fig. 9. Continuing the trend seen with the 5000 h electrode assemblies, the wt.% of C has further decreased to 40–45% (Fig. 9). The most plausible interpretation of this decrease in C weight concentration (or increase in Pt to C ratio) is a severe long term carbon corrosion and loss.

XPS results

PAFC assemblies were peeled apart, rinsed with ultra pure water and examined using XPS. Special care was required to delaminate the 16 000 h assemblies. For these electrode structures the surface of the cathode was scraped lightly to create an artificial break at the electrocatalyst-porous

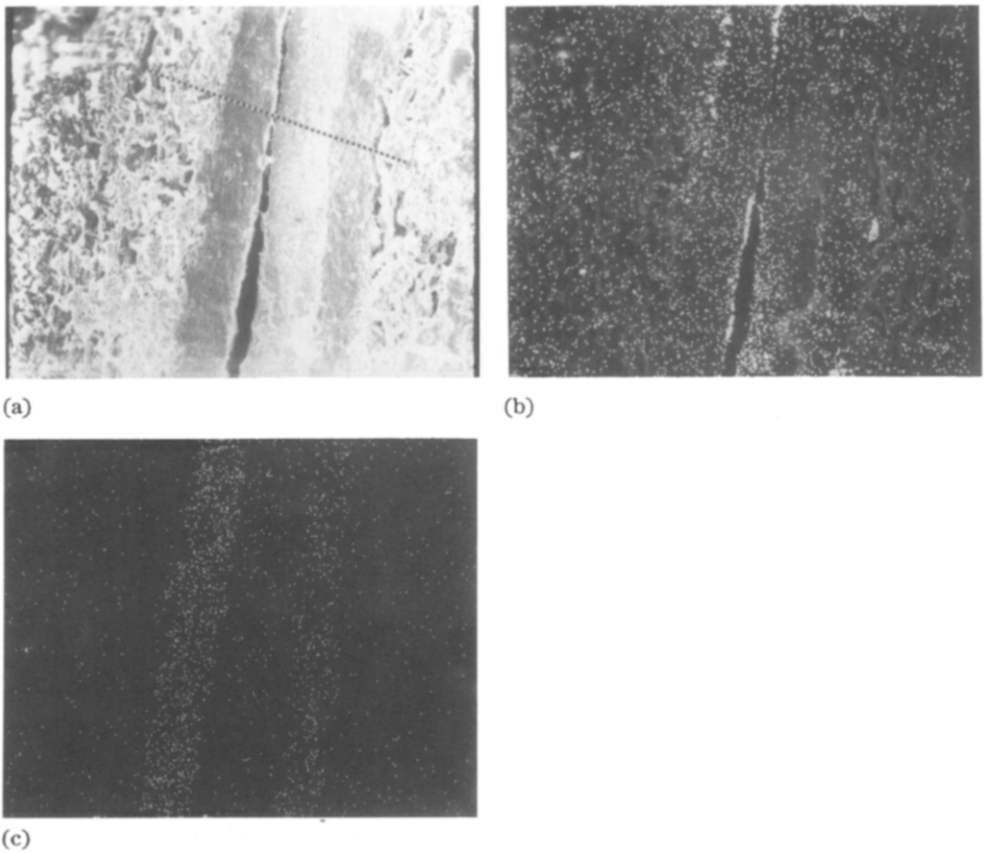

Fig. 8. (a) SEM of PAFC electrode assembly 8-3 operated for 16 000 h. Portions of the assembly are denoted. (b) Si X-ray fluorescence map over the same region as shown in (a). (c) Pt X-ray fluorescence image of the same region as in (b).

backing interface. The electrocatalyst layer was then peeled up and XPS spectra were recorded of the back side of the electrocatalyst layer. For all of the anode structures and for the reference and 5000 h cathodes the front side (side facing the anode) surface of the electrode was simply scraped to remove the tenacious SiC matrix. For these samples, however, some Si was always seen in the broadscan survey spectra that were run prior to recording the narrow regions for the analytical lines of interest. XPS is considerably more surface sensitive than EMP (analysis layer depth of ~50 Å versus 1–5 μm), and therefore, one should be aware of the different information content in each technique. Whereas EMP can provide quantitative elemental information for well behaved samples, XPS is used herein to analyze the chemical valency of specific elements present in the surface layer (e.g., C present as C, –CO, –COOH or – CF_x). No attempt was made to quantify the ratios of C to Pt using XPS because of the extremely low (but observable) levels of Pt. For the present samples, the C 1s energy region was specifically examined to shed light on the nature of loss of carbon in the electrocatalytic layers.

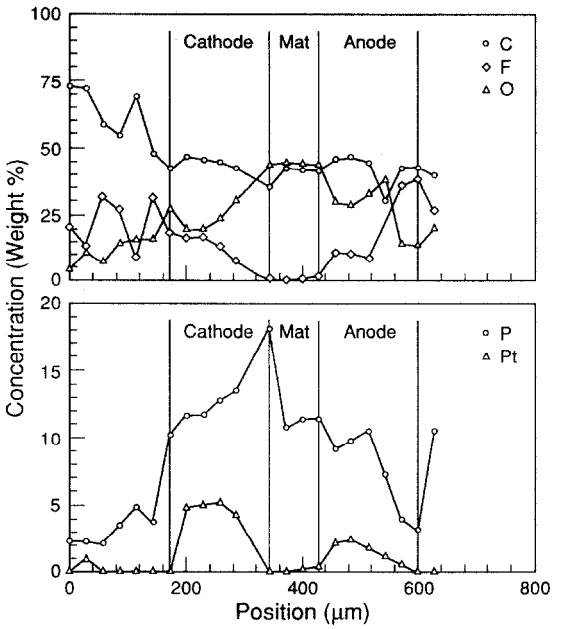

Fig. 9. Weight concentrations determined from the X-ray fluorescence along the line scan denoted in Fig. 8. Portions of the electrode assembly are denoted on the Fig.

The most informative XPS data are shown in Figs. 10 and 11. In Fig. 10, the C 1s lineshape for the reference anode and cathode is shown stack plotted with the corresponding data from 2-4 and 6-4 (5000 h) electrode structures. In the reference data note that there are two very distinct C 1s peaks appearing at 284.0 eV and approximately 291 eV binding energy. These two peaks are assigned to the carbon from electrocatalyst support and the Teflon blended into the structure, respectively. The peak arising from the Teflon component was noticed to shift dramatically, consistent with the Teflon particles charging during the XPS experiment. In most cases an electron flood gun was utilized to shift this feature to reported values [4]. The use of charge neutralization had a minimal effect on the C 1s feature arising from the graphite. The effect of charging on the C_{tef} can be seen in the spectrum recorded from the 2-4 cathode, where charge neutralization was not used. Other spectral features arising from –COH and –COOH functionalities can be fit to the region between the two prominent peaks. The ratio of the integrated intensity of the C_{tef} to C_{gr} peaks is 0.6 ± 0.1 for both the reference anode and cathode surfaces. Note that for both sets of data the used cathode electrode surfaces display a severe loss of intensity in the C_{gr} feature. For the 2-4 and 6-4 anode surfaces the C 1s spectral lineshape remains essentially the same as the reference data. In Fig. 11 a similar set is shown stack plotted for two of the 16 000 h electrode sets. The other two 16 000 h assemblies produced similar results and are not shown for brevity. Essentially the same result is seen in the C 1s spectra

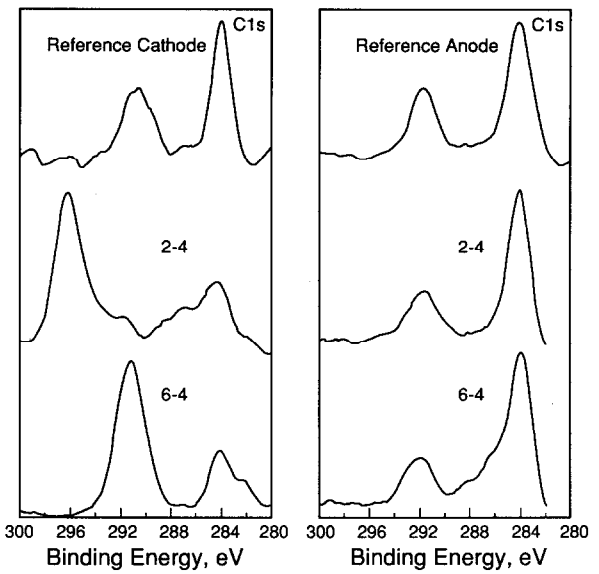

Fig. 10. X-ray photoelectron spectra (XPS) recorded over the C 1s region from the respective electrocatalyst layers (reference and 5000 h operated electrodes). The excitation source was an unmonochromatic Mg anode (1253.6 eV) and spectra were recorded at 50 eV pass energy. The C 1s contributions due to the graphite (284.6 eV) and Teflon (291 eV) are denoted on the Figure. The high binding energy of cathode assembly 2-4 is shown to illustrate the inherent charging of the Teflon particles (charge compensation was used in all of the other spectra).

as seen in the 5000 h electrodes, namely an extreme loss of the C_{gr} feature in the cathode electrocatalyst structures. These XPS results strongly indicate that the loss of carbon from the cathode is caused by graphite corrosion rather than by degradation of the teflon component.

TEM results

We used transmission electron microscopy (TEM) to observe the platinum particle size distribution in the cathodes. The TEM samples were prepared by scraping the cathodes with a scalpel over TEM grids and dropping petroleum ether on the grids. This spreads the cathode material and causes it to adhere to the grid. Figure 12 is a composite of reference cathode C381-2 and cathode 6-4. Generally, the platinum particles are much larger in the 5000 h and 16 000 h cathodes, than in the unused cathode. We did not do an extensive Pt particle size analysis in the TEM examination, although it is immediately apparent from inspection of Fig. 12 that the particle sizes have increased to approximately 200 Å after operation for 5000 h.

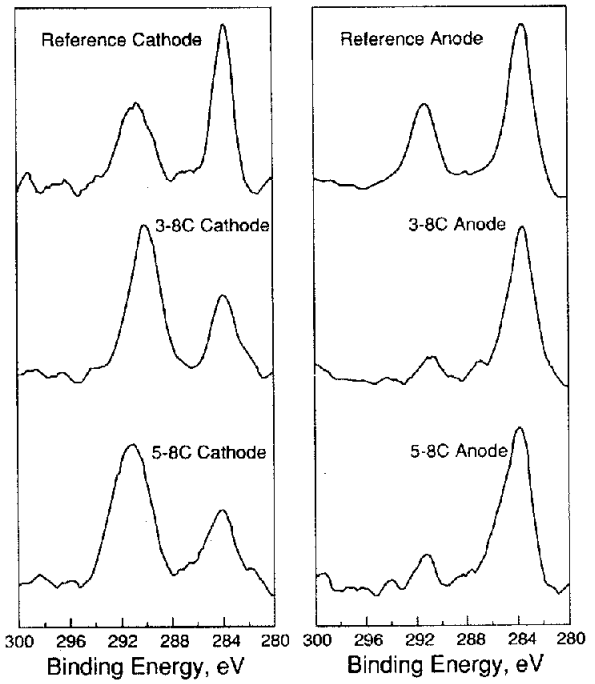

Fig. 11. XPS data recorded over the C 1s regions of PAFC electrocatalyst layers operated for 16 000 h. Other variables as in Fig. 10.

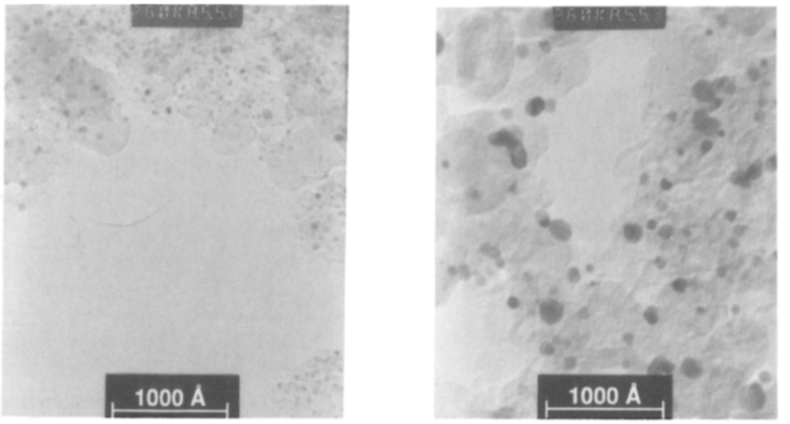

(a) (b)

Fig. 12. Transmission electron micrographs of (a) reference cathode and (b) 5000 h operated cathode electrocatalyst.

RBS results

Rutherford backscattering (RBS) was used to obtain depth profiles of the catalyst distributions. All these analyses were done with the ion beam

normal to the sample surface. We used 2 MeV alpha particles to obtain an accurate Pt/C ratio to a depth of 2×10^{19} atoms cm^{-2}, and 3 MeV protons to obtain profiles down to a depth of 10^{20} atoms cm^{-2}. The depth profiles are given on a scale of atoms cm^{-2} rather than on a distance scale, since the electrodes are rather porous, rough and the physical density of the material is not well defined. Despite this limitation, the Pt/C ratio is obtained by measuring the heights of the Pt and carbon edges and calculating the Pt/C ratio by using the known scattering cross sections for Pt and C. These cross sections are proportional to Z^2 so the Pt edge is extremely enhanced relative to the carbon edge. Figure 13(A) is an example of the RBS data for cathode 7-8-C (16 000 h). The solid line is a computer simulation with a Pt/C *atomic* ratio of 0.0297 (2.97%). The small edge around channel 260, 320 and 445 are for oxygen, fluorine and phosphorus, respectively. The key numbers are the heights of the platinum and carbon edges. Figure 13(B) and (C) display the same type of RBS data for a 5000 h cathode (cell 6-4) and the reference cathode (C381-2). The edge at channel 425 in Fig. 13(C) is from silicon. The Pt/C ratio for Fig. 13(B) is 1.45% and for Fig. 13(C) is 0.64%. RBS with 2 MeV alpha particles provides Pt/C atomic ratios with good accuracy, but only probes to a depth of 2×10^{19} atoms cm^{-2}. For deeper profiles (10^{20} atoms cm^{-2}), 3 MeV protons were used. The scattering at this energy for protons is not purely elastic (Rutherford) therefore the Pt/C ratio is somewhat inaccurate. Figure 14 is an example of a proton RBS spectrum for cathode 3-8-C. It shows that the Pt distribution is relatively constant to a depth of 10^{20} atoms cm^{-2}. No information can be gained on the atomic ratios since for the lighter elements (C, O, F) the scattering is non-Rutherford; that is, it has a significant contribution from nuclear effects. Figure 15 summarizes the Pt/C atomic concentration ratios for the cathodes measured. Note that there is a very significant increase in the Pt/C ratio with operating time for all of the 16 000 h cathodes which we interpret as a carbon loss.

Discussion

An extensive data base on carbon corrosion exists in the electrochemical fuel cell literature [5]. In general, the relative kinetic inertness of a variety of carbon types has been experimentally verified [5] and in general accounts for the widespread use of a variety of carbon types as electrocatalyst supports. Work by Kinoshita [6] on the corrosion of carbon under PAFC operation conditions has previously demonstrated that for short term operation the Pt electrocatalyst did not have an effect on the net carbon corrosion rate. However, in a study of carbon corrosion in alkaline solutions, Ross and Sokol [7] have previously demonstrated that a supported Co oxide electrocatalyst produced a notable increase in the overall carbon corrosion process when compared to the bare carbon corrosion rate. Corrosion of the carbon electrocatalyst support under long term PAFC operation conditions appears

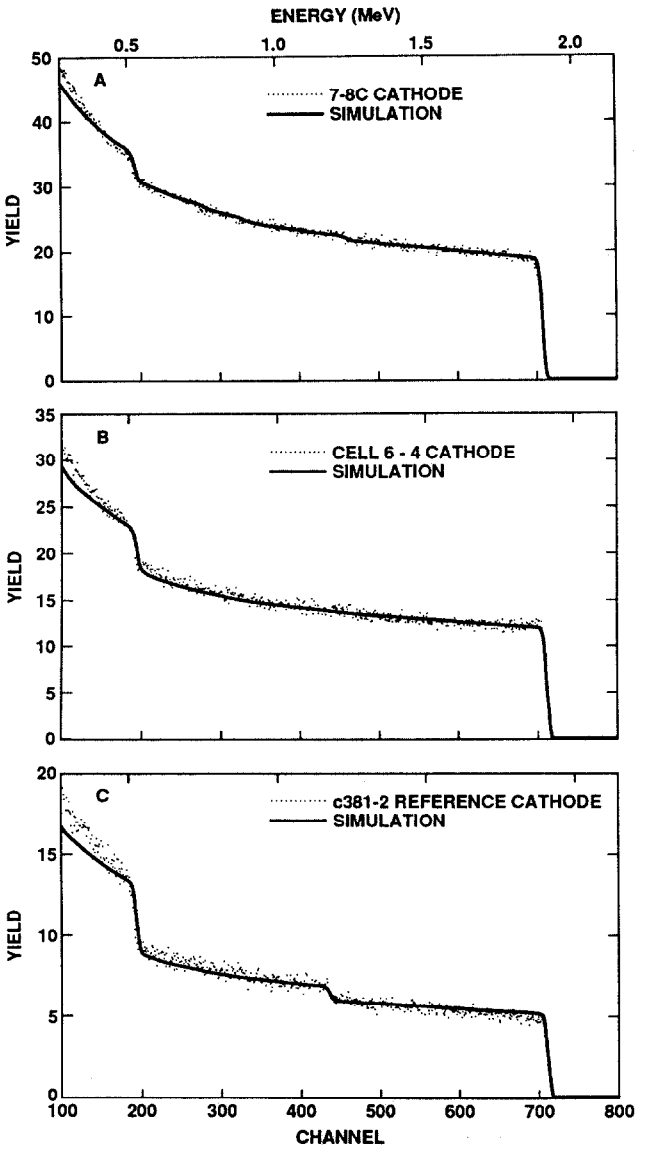

Fig. 13. (A) Rutherford backscattered spectrum (RBS) recorded from 16 000 h operated cathode electrocatalyst layer. The incident ion was 2.0 MeV alpha particles. Composition of the assemblies was accomplished using the RUMP code as described in text and the fit is shown on the Fig. (B) Same as (A) except for a 5000 h operated cathode electrocatalyst layer. (C) Same as (A) except recorded from a reference cathode electrocatalyst layer.

to be a subject that has been widely noted but not extensively reported in the electrochemical community.

The change in Pt catalyst distribution following long term PAFC operation has been studied by Aragone *et al.* [8] using EMP and TEM methods and

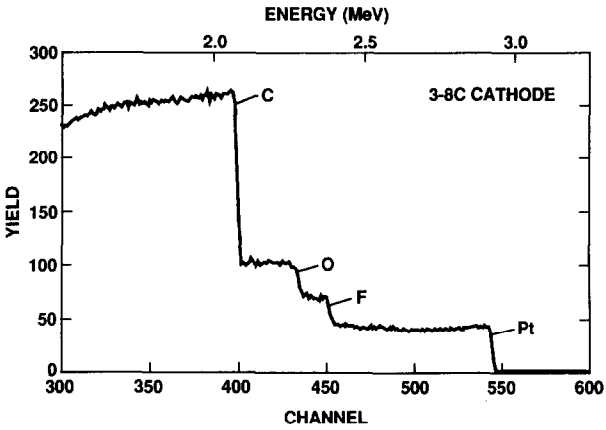

Fig. 14. RBS spectrum recorded from a 5000 h cathode electrocatalyst layer using 3.0 MeV protons. The elemental edges are denoted.

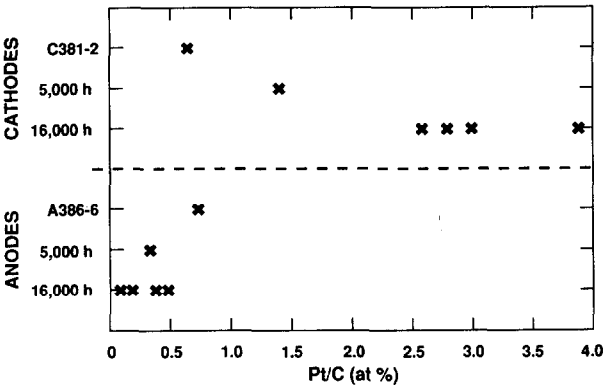

Fig. 15. The Pt/C ratio determined from the RBS data analysis for various anode and cathode electrocatalyst layers.

by Hyde *et al.* [9] using particle induced X-ray emission and RBS methods. In both cases the corrosion of Pt was noted to be quite severe at the cathode front surface, and was followed by migration of the Pt through the cell and its redeposition at the PAFC anode front surface. Previous RBS work from this laboratory using a Pt cathode and a Pd anode in PAFC single cells has demonstrated this corrosion and migration of Pt through the cell assembly [10]. These observations of Pt corrosion and migration point to the very careful control that PAFC assemblies require during their operational history. Any open circuit condition at high temperature, however short in duration, produces the serious observed cathode Pt corrosion and migration problems.

In view of these previous studies, and from the results obtained in the characterization of the PAFC assemblies of this work, we can summarize as follows.

(1) The profiles of the catalyst in both the anode and the cathode layer did not show any preferential loss or peaking. This shows that because of the quality of the fabricated catalyst and the mode of operation of the stack during the long term testing, loss of Pt from the cathode catalyst, and Pt redeposition on the front surface of the anode, was not detected, even after about 16 000 h of testing. This aspect is stressed because the pattern of Pt migration from cathode to the front surface of the anode in operating PAFCs has been identified in the past in several similar analytical efforts [8–10], and it was gratifying to find out that it did not take place in the Westinghouse cells examined. This is a testament to the operational control and procedures implemented in the operation of the Westinghouse PAFC stack.

(2) The most pronounced change in cell composition detected following testing for 5000 and 16 000 h was the increase in Pt/C ratio. This was clearly detected with both the EMP and the RBS techniques. Since the latter is the more quantitative tool (though associated with a smaller penetration depth), further discussion is based upon RBS results presented in Fig. 15. These results show an increase in Pt/C ratio in the cathode by about a factor of 3 after 5000 h and by a factor of 5–6 after 16 000 h. Assuming that the loss of Pt is relatively small, as concluded from the lack of any indication of Pt migration to the anode and only a low level of Pt found in the mat layer (see below) the only way to interpret this increase in Pt/C ratio is by the loss of carbon. This loss is, however, very substantial. If the initial concentration of Pt in the cathode catalyst is 10% an increase in the ratio Pt/C by a factor of 6 means a loss of about 80% of the carbon (!) from the cathode catalyst layer after 16 000 h. This behavior is clearly unique for the cathode catalyst, whereas the anode catalyst layer maintains the same ratio of Pt:C following the 16 000 h of operation (Fig. 15). This clearly demonstrates that the loss of carbon occurs by an electrochemical mechanism and is enhanced at the higher potentials experienced by the air cathode in the fuel cell. A direct correlation between the severe loss of carbon from the cathode catalyst and the continuous loss of cell voltage in this stack (*c.* 8 mV/1000 h) could not be established by the analytical results presented here alone. However, it would be surprising if a loss of 80% of the mass of the carbon in the cathode catalyst layer could take place without any consequence. Indeed, it is quite amazing that after having lost 80% of the carbon in the carbon in the cathode catalyst layer, the cell is functioning with a loss of only 130 mV in voltage. The explanation for this surprising preservation of cell performance may be that the mechanical pressure continously applied across the cells allows the maintainence of a reasonable electronic connectivity within the shrinking catalyst layer, even following such a severe carbon loss. These results suggest an obvious R&D effort on searching for carbon materials with lower electrochemical corrosion rates.

(3) The XPS results in this report help to clarify the nature of the increase in Pt/C ratio in the cathode catalyst layer. These results have the advantage of distinguishing clearly between carbon associated with the catalyst support (XC-72) and the carbon in the Teflon additive. The XPS results could thus prove in an unequivocal way that the carbon lost is from the support material – not from the Teflon.

(4) A small level of Pt, estimated at 15% of the overall initial loading, is found in the mat layer after 5000 h (and somewhat more after 16 000 h), according to both the EMP and the RBS results.

(5) The TEM results presented in Fig. 12 clearly demonstrate the well recognized phenomenon of Pt particle agglomeration in the cathode catalyst layer, which is seen to be quite substantial after 5000 h of stack operation. This is obviously a process that could contribute to performance loss.

(6) The mechanical integrity of the assemblies was found to be quite satisfactory after 5000 h, but much less so after 16 000 h. In particular, SiC has been very difficult to detect in the samples run for 16 000 h.

Acknowledgement

The work at Los Alamos was supported by the Morgantown Energy Technology Center and is gratefully acknowledged.

References

1 J. M. Feret, M. K. Wright, L. L. France, J. L. Kelley, A. J. Pereira and A. Kush, *Proc. First Annual Fuel Cells Contractors Meet., DOE/METC-89/6105*, 1989, p. 287.
2 A. J. Appleby, in S. S. Penner, (ed.), *Energy (Special Issue) 11*, Pergamon, New York, 1986.
3 L. Feldman and J. W. Mayer, *Fundamentals of Surface and Thin Film Analysis*, North-Holland, New York, 1986, Ch. 10.
4 C. D. Wagner, W. M. Riggs, L. E. Davis, J. F. Moulder and G. E. Muilenberg, *Handbook of X-ray Photoelectron Spectroscopy*, Perkin-Elmer Corp., Physical Electronics Division, Eden Prairie, MN, 1979.
5 A. J. Appleby, in *Electrochemical Society Proceedings*, Vol. 84-5, *The Electrochemistry of Carbon*, The Electrochemical Society, Pennington, NJ, 1984, p. 251, and refs. therein.
6 K. Kinoshita, *Electrochemical Society Proceedings*, Vol. 84-5, *The Electrochemistry of Carbon*, The Electrochemical Society, Pennington, NJ, 1984, p. 273.
7 P. N. Ross and H. Sokol, *J. Electrochem. Soc., 131* (1984) 1742.
8 J. Aragane, T. Murahashi and T. Odaka, *J. Electrochem. Soc., 135* (1988) 844.
9 P. J. Hyde, C. J. Maggiore and S. Srinivasan, *J. Electroanal. Chem., 168* (1984) 383.
10 L. Borodovsky, J. G. Beery and M. T. Paffett, *Nucl. Instrum. Methods* in *Phys. Res. B, 24/25* (1987) 568.